

Nonlinear rotation-invariant pattern recognition by use of the optical morphological correlation

Pascuala Garcia-Martinez, Carlos Ferreira, Javier Garcia, and Henri H. Arsenault

We introduce a modification of the nonlinear morphological correlation for optical rotation-invariant pattern recognition. The high selectivity of the morphological correlation is conserved compared with standard linear correlation. The operation performs the common morphological correlation by extraction of the information by means of a circular-harmonic component of a reference. In spite of some loss of information good discrimination is obtained, especially for detecting images with a high degree of resemblance. Computer simulations are presented, as well as optical experiments implemented with a joint transform correlator. © 2000 Optical Society of America

OCIS codes: 100.4550, 070.4340, 070.5010.

1. Introduction

The common cross correlation is used widely in image processing, especially for image detection.¹ The matched filter is optimum in the sense that it minimizes the mean-squared error of the signal-to-noise ratio of the output. Minimizing this error criterion is equivalent to maximizing the linear cross correlation. The operation can be performed optically, and it has been used widely in several optical areas.² One application is the detection of images distorted by rotation,^{3,4} scale,⁵ or projection⁶ changes.

For rotation-invariant pattern recognition circular-harmonic component (CHC) decomposition has been used extensively.^{3,4} Hence the linear correlation between an image and the CHC of a reference object provides rotation-invariant recognition. It can be performed optically by means of the classical linear correlator⁷ or the joint transform correlator⁸ (JTC). The linear nature of the cross correlation is one of its important attributes. For some pattern-recognition tasks it might be required to detect a dark rotated object in the presence of a bright background or of bright patterns. In this case the linear correlation

can give rise to false alarms. Therefore other nonlinear correlation methods are sometimes more appropriate for such cases.

Nonlinear morphological correlation (MC) has been shown to be an important tool for optical pattern recognition.^{9,10} The nonlinear property of this operation and the possibility of optical implementations make it attractive for identifying objects that have different orientations. However, MC does not provide detection with rotation invariance. To achieve this, we propose a modification of this nonlinear correlation and introduce an enhanced MC that we call rotation-invariant morphological correlation (RIMC). It also offers, in addition to a high discrimination capability for detecting images with high resemblance, robust rotation-invariant detection for low-intensity images in the presence of high-intensity patterns to be rejected.

2. Morphological Correlation

Let us consider two real-valued two-dimensional discrete signals represented by $f(\zeta, \eta)$ and $g(\zeta, \eta)$, where $(\zeta, \eta) \in \mathbb{Z}^2$. Assume that f is a pattern to be detected in the presence of g . For finding which shifted version of f best matches g one powerful approach has been to search for the shift lag (x, y) that minimizes the mean absolute error (MAE):

$$\text{MAE}(x, y) = \sum_{\zeta, \eta \in W} |g(\zeta + x, \eta + y) - f(\zeta, \eta)|. \quad (1)$$

Maragos¹¹ introduced the MC as a robust detection method that minimizes the MAE. MC provides a better performance and an improved discrimination

P. Garcia-Martinez, C. Ferreira, and J. Garcia are with the Departament d'Òptica, Universitat de Valencia, Calle Dr. Moliner 50, 46100 Burjassot, Spain. P. Garcia-Martinez is also with and H. H. Arsenault (arseno@phy.ulaval.ca) is with the Department de Physiques, Centre d'Optique, Photonique et Lasers, Université Laval, Ste. Foy, G1K 7P4 Québec, Canada.

Received 14 May 1999; revised manuscript received 16 August 1999.

0003-6935/00/050776-06\$15.00/0

© 2000 Optical Society of America

capability over linear correlation for pattern-recognition tasks. In the manner of Ref. 11 and under certain assumptions minimizing the MAE is equivalent to maximizing a nonlinear cross correlation, defined as

$$\mu_{gf}(x, y) = \sum_{\zeta, \eta \in W} \min[g(\zeta + x, \eta + y), f(\zeta, \eta)], \quad (2)$$

which is the definition of the MC given by Maragos. In Ref. 11 it was shown that the MC between the functions g and f is the average over all amplitudes of the linear correlation between thresholded versions of g , $[g_q(x, y)]$ and f , $[f_q(x, y)]$ for every gray-level value q . When g and f are quantized gray-level images Eq. (2) can be written as

$$\begin{aligned} \mu_{gf}(x, y) &= \sum_{q=1}^{Q-1} \mu_{g_q f_q}(x, y) \\ &= \sum_{q=1}^{Q-1} \gamma_{g_q f_q}(x, y) \\ &= \sum_{q=1}^{Q-1} [g_q \otimes f_q](x, y), \end{aligned} \quad (3)$$

where Q is the number of gray levels of the images, $\mu_{g_q f_q}(x, y)$ is the MC between the q th binary slices $g_q(x, y)$ and $f_q(x, y)$, $\gamma_{g_q f_q}(x, y)$ is the linear correlation between the same binary slices, and the symbol \otimes denotes linear correlation.

The optical implementation of the MC is carried out by means of a JTC scheme,⁸ as illustrated in Fig. 1. The nonlinearity provides as a bonus the detection of low-intensity images in the presence of high-intensity patterns. With this optoelectronic system the sum of the amplitude-correlation outputs of Eq. (3) is obtained. To implement this nonlinear operation, we calculate the joint power spectrum JPS_q of each binary slice.⁹ The sum obtained is

$$\begin{aligned} \text{JPS}_2(u, v) &= \sum_{q=1}^{Q-1} \text{JPS}_q(u, v) \\ &= \sum_{q=1}^{Q-1} |F_q(u, v)|^2 + \sum_{q=1}^{Q-1} |G_q(u, v)|^2 \\ &\quad + \sum_{q=1}^{Q-1} F_q^*(u, v) G_q(u, v) \exp[-i2\phi_q(u, v)] \\ &\quad + \sum_{q=1}^{Q-1} F_q(u, v) G_q^*(u, v) \exp[i2\phi_q(u, v)]. \end{aligned} \quad (4)$$

Note that the Fourier transforms (FT's) of both the third and the fourth terms on the right-hand side of Eq. (4) yield the MC between the scene $g(x, y)$ and the reference $f(x, y)$.

3. Rotation-Invariant Linear Correlation

Circular-harmonic (CH) expansion has been used widely for rotation-invariant pattern recognition.^{3,4}

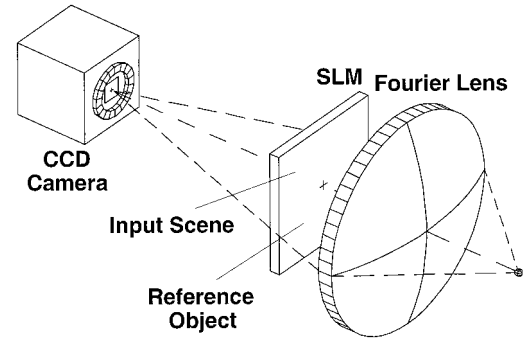


Fig. 1. JTC setup. SLM, spatial light modulator.

The expansion of the function $f(r, \theta)$ expressed in polar coordinates can be written as

$$f(r, \theta) = \sum_{m=-\infty}^{\infty} f_m(r) \exp(im\theta), \quad (5)$$

where

$$f_m(r) = \int_0^{2\pi} f(r, \theta) \exp(-im\theta) d\theta, \quad (6)$$

with m as the order of the CHC and $i = \sigma_{-1}$. The CH filter (CHF), introduced by Hsu *et al.*,^{3,4} provides full rotation invariance in addition to shift invariance. Usually, the CHF uses one m th-order component $f_m(r) \exp(im\theta)$ of the CH expansion of the object $f(r, \theta)$ to carry out a linear correlation and also to achieve rotation-invariant pattern recognition.

The performance of the CHF involves both the order of the CHC and the expansion center chosen for the change of Cartesian coordinates into polar coordinates. Several methods have been introduced to select the appropriate order and center, called the proper center.^{12,13} Both the order m and the best center of expansion depend on the geometry of the object. In Refs. 12 and 13, the choice is based on the energy map of the CHC's, but that energy is not the only parameter to be considered in correlation. We later proposed a method to select the proper center that is based on combining the information from both the energy and a correlation parameter called the peak-to-correlation energy¹⁴ (PCE).

One can achieve rotation-invariant detection by carrying out the correlation between a scene $g(r, \theta)$ and a CHC $f_m(r, \theta)$ (Refs. 3 and 4):

$$\gamma_m(r, \theta) = g(r, \theta) \otimes f_m(r, \theta), \quad (7)$$

where the symbol \otimes denotes linear correlation.

Conventional matched-filtering systems use all the CHC's of the target as the reference with the result that the rotation problem appears. The CHF is a linear filter and is therefore shift invariant, like the conventional matched filter. The CHF matches a single CHC of the target, resulting in rotation invariance.³ There are also other kind of filters matched to more than one CHC, but, although they provide much better discrimination, the invariant property is lost.

4. Rotation-Invariant Nonlinear Correlation

Because the MC yields better pattern-recognition performance than does linear correlation and because it is suitable for optical implementation, we use it to recognize objects with different orientations. In Eq. (3) assume that each q -binary slice of the reference object $f_q(r, \theta)$ can be decomposed into CH functions:

$$\begin{aligned} \mu(r, \theta) &= \sum_{q=1}^{Q-1} g_q(r, \theta) \otimes f_q(r, \theta) \\ &\times \sum_{q=1}^{Q-1} \left[g_q(r, \theta) \otimes \sum_{m=-\infty}^{\infty} f_{q_m}(r, \theta) \right] \\ &\times \sum_{m=-\infty}^{\infty} \sum_{q=1}^{Q-1} [g_q(r, \theta) \otimes f_{q_m}(r, \theta)]. \quad (8) \end{aligned}$$

Note that, in Eq. (8), the spatial coordinates have been changed from those of Eq. (3). Rotation-invariant pattern recognition can be achieved by use of only one component of the CH decomposition and then performance of the linear correlation. If only one CHC is used for each q correlation in Eq. (8) the nonlinear correlation will permit the detection of a target for any angular orientation. This means that other nonlinear correlations based on the MC could be devised. So, taking into account the previous argument and using only one m th-order CHC in Eq. (8), we call this correlation the RIMC, defined as

$$\tilde{\mu}_{gf}^m(r, \theta) = \sum_{q=1}^{Q-1} g_q(r, \theta) \otimes f_{q_m}(r, \theta). \quad (9)$$

The correlation $\tilde{\mu}_{gf}^m(r, \theta)$ is also a nonlinear correlation, inspired by the MC.^{9,10} The difference between $\tilde{\mu}_{gf}^m(r, \theta)$ (the RIMC) and $\mu_{gf}(r, \theta)$ (the MC) is that, for the RIMC, only part, $f_{q_m}(x, y)$, of the thresholded reference object $f_q(x, y)$ is used instead of the total information of $f_q(x, y)$ that is used for the MC.

5. Simulation Results

In this section, we present some computer simulations to compare the linear correlation with the MC and its applications to rotation-invariant pattern recognition. Figure 2 shows an input scene that is made up of two different kinds of objects: The reference object is the dark object marked with an arrow, and the bright lower one is an object to be rejected. To perform pattern recognition with rotation invariance, it is necessary that the reference object be rotated by 90°.

The choices of the order and of the expansion center are important both for the CHC in the linear case and for the RIMC case. In Eq. (7) the function $f_m(x, y)$ takes into account the choice of the CH order and of the expansion center, as was discussed elsewhere.^{12,14} In Ref. 14, both the energy and the PCE maps of the gray-level reference object are calculated, and the maximum of the PCE map that also has a high value in the energy map is selected. This process ensures both a sharp correlation-peak shape and a high PCE value.

For the RIMC the CHC's of the q th binary slices of

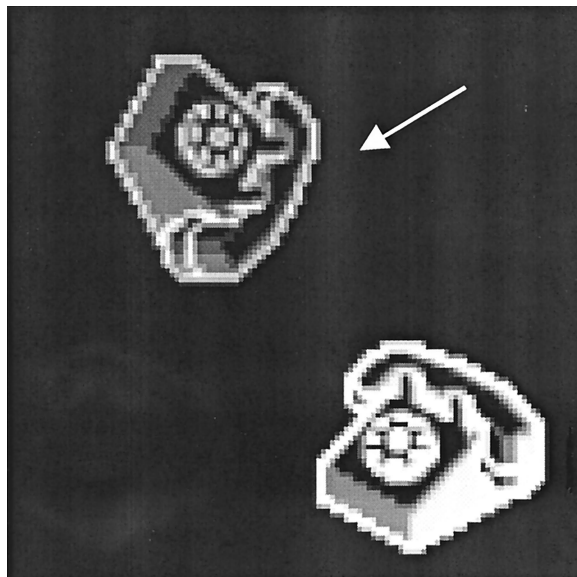


Fig. 2. Input scene with the reference object rotated by 90°. The object in the lower right-hand corner is to be rejected.

the reference-object versions are required. We chose the same expansion order as for the linear case because that parameter is strongly dependent on the geometry of the reference object and also because the shape of each binary slice depends strongly on the shape of the reference object. For the expansion center, we assumed that all the expansion centers occur about the center of mass of the reference object because the energy distribution is strongly related to that mass center. So, to perform the RIMC, we select the center of mass of the reference object as the expansion center for all the q th binary-slice CHC's. For the objects shown in Fig. 2, we used $m = 3$ CHF's.

The linear correlation for an $m = 3$ CHF is shown in Fig. 3. Note that this operation is not capable of detecting the reference object, and a false alarm appears. On the other hand, if we use the same input scene with the RIMC, we obtain the correlation output shown in Fig. 4. We used the $m = 3$ CHF order for each binary slice. Now we detect the rotated version of the reference object, and a threshold value of 50% is enough to reject the false alarm.

These computer simulations demonstrate the improved performance of the RIMC over the CHC linear correlation. The next step is to perform the optical implementation. To implement the RIMC, we need to take into account that the CHC filter is a complex function and that it may be difficult to introduce complex values in the JTC. We propose some ideas for using the CHF in Section 6.

6. Experimental System

The optical implementation of the RIMC can be carried out in a manner similar to that used for the optical implementation of the MC.⁹ As we indicated in Section 2, a JTC scheme was used to implement the nonlinear correlation optically. The JTC displays both the input scene and the reference object in

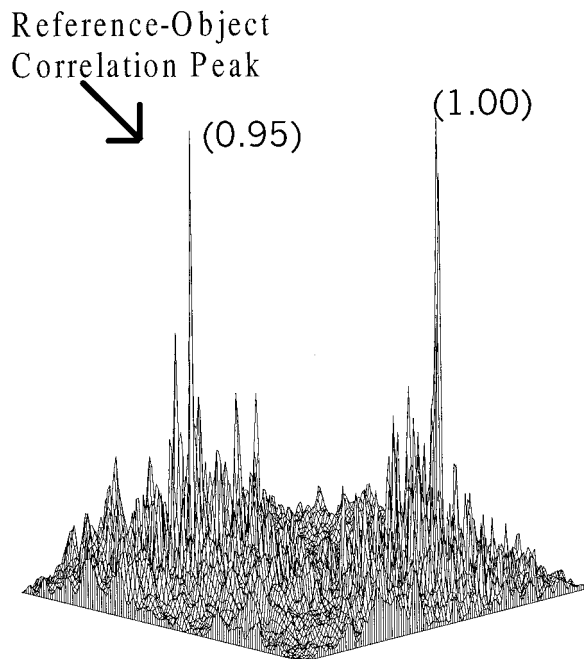


Fig. 3. Rotation-invariant correlation by use of a third-order CHF.

a spatial light modulator. A first FT gives the JPS. A second FT yields the correlation output.⁸ The JTC scheme is shown in Fig. 1.

The JTC usually is implemented with real and positive inputs and references, but CHF's are complex functions [see Eq. (5)]. Yu *et al.*¹⁵ showed that, by use of the real and the imaginary parts of a CH function as two separate positive reference objects in

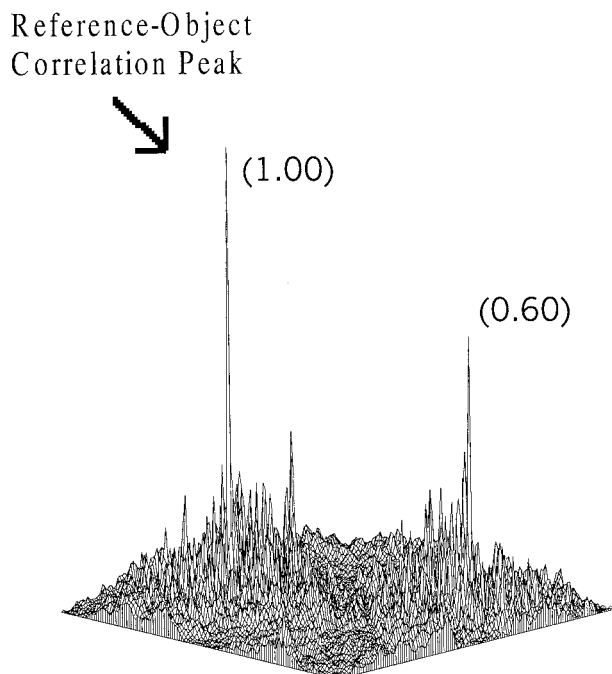


Fig. 4. Rotation MC by use of a third-order CH.

a JTC setup, rotation- and shift-invariant pattern recognition can be achieved. This approach is based on a digital postprocessing step that adds two correlation peaks, one for the real part of the CH and the other for the imaginary part. This scheme also permits the determination of the angular orientation of the input by evaluation of the ratio of the two correlations.

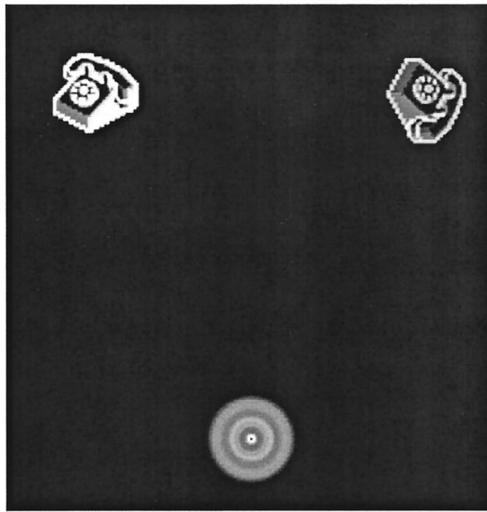
Methods based on recording the phase as well as the amplitude information of the reference object by their encoding on a grating were also proposed.¹⁶ The input object, placed side by side with this reference, is multiplied by a grating so that the joint transform distribution is located at the first diffraction order. However, this approach requires holographic methods for complex-valued functions. Some approaches that are based on representing complex-valued functions by their decomposition in three positive-valued components can overcome those drawbacks.¹⁷ However, this process is difficult to implement with either coherent or incoherent illumination. It would be useful not only for optical techniques but also for digital techniques if a rotation-invariant real filter could be found. Arsenault *et al.*¹⁸ have developed real rotation-invariant filters, but only partial rotation invariance was achieved.

Yang *et al.*¹⁹ proposed an optimum circular filter for rotation-invariant pattern recognition on the basis of an angular average of matched filters. The filter was later recognized to be the $m = 0$ component of the CH expansion. This filter is real and positive, but, although rotation invariance is achieved, the reference-object information contained in the filter is reduced.

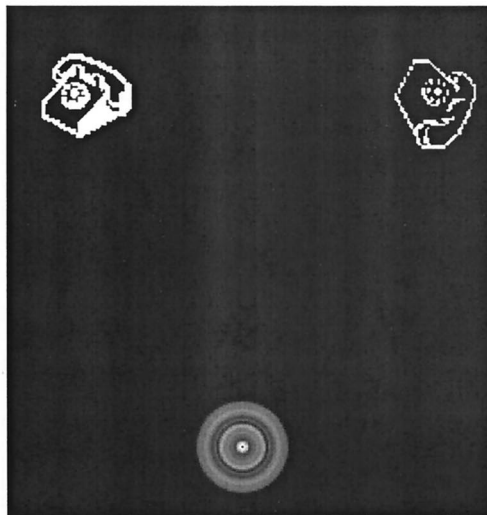
Because of the real and positive mathematical nature of the $m = 0$ CH, we used the zero-order CH with the RIMC to achieve rotation-invariant image detection for the optical experiments. Now we display both the input scene and the $m = 0$ CHC of the reference object to obtain the JPS_q^{CH} for each binary slice. With the similarity to Eq. (9) taken into account the resulting distributions are added as

$$\begin{aligned}
 JPS_{\Sigma}^{CH}(u, v) &= \sum_{q=1}^{Q-1} JPS_q^{CH}(u, v) \\
 &= \sum_{q=1}^{Q-1} |F_{q_{m=0}}(u, v)|^2 + \sum_{q=1}^{Q-1} |G_q(u, v)|^2 \\
 &\quad + \sum_{q=1}^{Q-1} F_{q_{m=0}}^*(u, v) G_q(u, v) \\
 &\quad \times \exp[-i2\phi_{q_{m=0}}(u, v)] \\
 &\quad + \sum_{q=1}^{Q-1} F_{q_{m=0}}(u, v) G_q^*(u, v) \\
 &\quad \times \exp[i2\phi_{q_{m=0}}(u, v)]. \tag{10}
 \end{aligned}$$

Note that the FT's of the third and the fourth terms on the right-hand side yield the RIMC between the scene $g(x, y)$ and the reference object $f(x, y)$ and that the result is rotation invariant.



(a)



(b)

Fig. 5. (a) Joint input scene for the optical linear correlation and (b) a q -sliced joint input scene for the optical RIMC.

7. Optical Results

For demonstrating the advantages of the RIMC for rotation-invariant pattern detection optical experiments were performed by use of a JTC architecture. The optical experiments compare results for the linear correlation and for the nonlinear RIMC.

We used a Kopin LVGA active-matrix liquid-crystal display. This device has a VGA display, an active-matrix liquid-crystal display with single-crystal silicon integrated drivers and a monochromatic analog gray scale. An image size of 640×480 pixels displays the input scene. We used a 12-bit CCD camera to capture the JPS_q^{CH} .

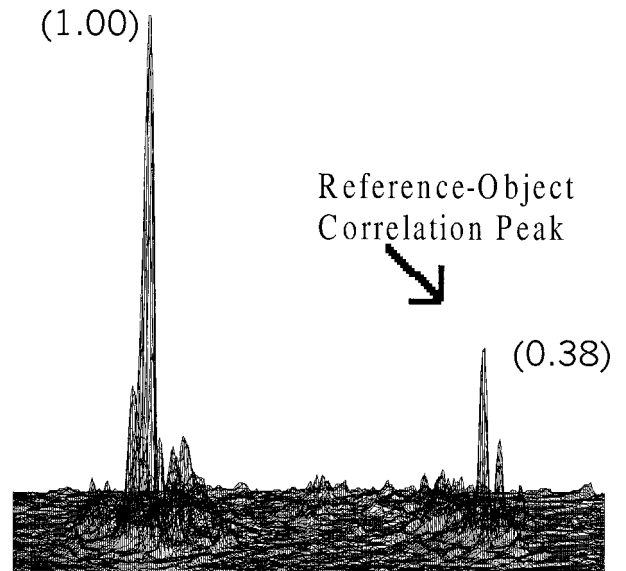


Fig. 6. Three-dimensional plots of the optical correlation output for linear correlation: a false alarm occurs. The normalized correlation-peak values are shown.

To carry out the optical linear correlation between an input scene and the zero-order CHC of the reference object, we introduce both distributions in the input plane of the JTC, as illustrated in Fig. 5(a). To obtain the RIMC optically, we binarized the input scene and calculated the $m = 0$ CHC of the thresholded reference object. We chose the center of mass of the reference object as the center of expansion. Figure 5(b) shows one joint input slice. The JPS_q^{CH} was obtained for all slices. The summation of all the JPS_q^{CH} values was performed electronically and

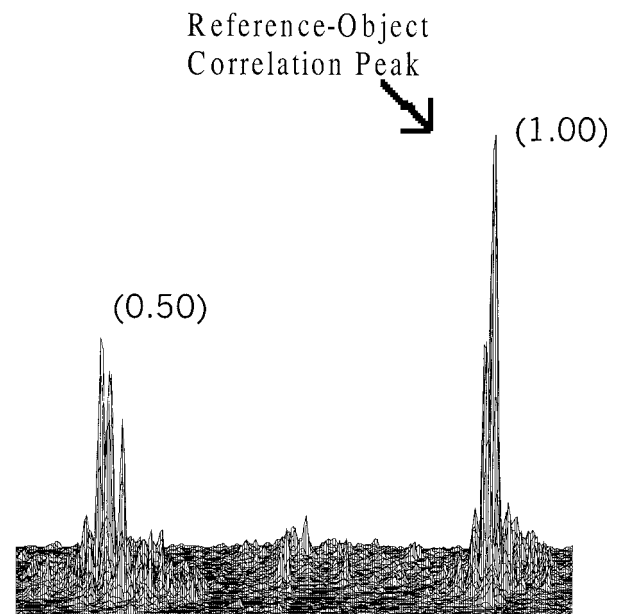


Fig. 7. Three-dimensional plots of the optical correlation output for the RIMC: no false alarm occurs. The normalized correlation-peak values are shown.

readdressed to the input plane. A final FT yielded the nonlinear RIMC.

In our optical setup, we blocked the dc term by using a black spot to enhance the high-frequency components. This method is used widely in JTC implementations. There are other methods for simulating high-pass filtering.

The three-dimensional correlation plots obtained for both the linear correlation and the RIMC are shown in Figs. 6 and 7, respectively. Because of its nonlinearity, the RIMC yields a higher peak for the dark object, so correct detection is obtained. However, the normal correlation yields a higher peak for the bright object.

8. Conclusion

The RIMC yields rotation-invariant pattern recognition. This nonlinear correlation has been implemented optically. The main advantage of this nonlinear operation is the provision of efficient rotation-invariant low-intensity image detection in the presence of other high-intensity patterns. The nonlinearity of the process permits rotation-invariant detection for cases in which the low intensity of false targets degrades normal correlation results.

This research was supported by the Spanish DGES (Dirección General de Enseñanza Superior) under project PB96-1134-C02-02 and by a grant from the Fonds pour la Formation de Chercheurs et l'Aide à la Recherche, Québec, Canada. P. Garcia-Martinez acknowledges a postdoctoral grant from the Secretaría de Estado de Universidades.

References

1. R. O. Duda and P. E. Hart, *Pattern Classification and Scene Analysis* (Wiley, New York, 1973), Chap. 8.
2. J. W. Goodman, *Introduction to Fourier Optics*, 2nd ed. (McGraw-Hill, New York, 1996).
3. Y. N. Hsu, H. H. Arsenault, and G. April, "Rotation-invariant digital pattern recognition using circular-harmonic expansion," *Appl. Opt.* **21**, 4012–4015 (1982).

4. Y. N. Hsu and H. H. Arsenault, "Optical pattern recognition using circular-harmonic expansion," *Appl. Opt.* **21**, 4016–4019 (1982).
5. D. Casasent and D. Psaltis, "Scale-invariant optical transform," *Opt. Eng.* **15**, 258–261 (1976).
6. D. Mendlovic, N. Konforti, and E. Marom, "Shift- and projection-invariant pattern recognition," *Appl. Opt.* **28**, 4784–4789 (1990).
7. A. VanderLugt, "Signal detection by complex spatial filtering," *IEEE Trans. Inf. Theory* **IT-10**, 139–145 (1964).
8. C. S. Weaver and J. W. Goodman, "Technique for optically convolving two functions," *Appl. Opt.* **5**, 1248–1249 (1966).
9. P. Garcia-Martinez, D. Mas, J. Garcia, and C. Ferreira, "Non-linear morphological correlation: optoelectronic implementation," *Appl. Opt.* **37**, 2112–2118 (1998).
10. A. Shemer, D. Mendlovic, G. Shabtay, P. Garcia-Martinez, and J. Garcia, "Modified morphological correlation based on bit-map representation," *Appl. Opt.* **38**, 781–787 (1999).
11. P. Maragos and R. W. Shafer, "Morphological systems for multidimensional signal processing," *Proc. IEEE* **78**, 894–902 (1982).
12. Y. Sheng and H. H. Arsenault, "Method of determining expansion centers and predicting circular-harmonic filters," *J. Opt. Soc. Am. A* **4**, 1793–1797 (1987).
13. G. Premont and Y. Sheng, "Fast design of circular-harmonic filters using simulated annealing," *Appl. Opt.* **32**, 3116–3121 (1993).
14. P. Garcia-Martinez, J. Garcia, and C. Ferreira, "A new criterion for determining the expansion center for circular-harmonic filters," *Opt. Commun.* **117**, 399–405 (1995).
15. F. T. S. Yu, X. Li, E. Tam, S. Jutamulia, and D. A. Gregory, "Rotation-invariant pattern recognition with a programmable joint transform correlator," *Appl. Opt.* **28**, 4725–4727 (1989).
16. D. Mendlovic, E. Marom, and N. Konforti, "Complex-reference joint transform correlator," *Opt. Lett.* **15**, 1224–1226 (1990).
17. R. Pierstun, J. Rosen, and J. Shamir, "Generation of continuous complex-valued functions of a joint transform correlator," *Appl. Opt.* **33**, 4398–4405 (1994).
18. H. H. Arsenault, C. Ferreira, M. P. Levesque, and T. Szoplik, "Simpler filter with limited rotation invariance," *Appl. Opt.* **25**, 3230–3234 (1986).
19. Y. Yang, Y. N. Hsu, and H. H. Arsenault, "Optimum circular symmetrical filters and their uses in pattern recognition," *Opt. Acta* **29**, 627–644 (1982).